# Performance of Crossed Long-Gauge Strain Sensors in the Spread Footing Foundation

YITIAN LIANG and BRANKO GLISIC

## ABSTRACT

Estimations of shear stresses are essential design procedures of spread footing foundations and detecting shear strain at critical planes is crucial in structural health monitoring because it provides valuable insights into the structural stability of the foundation. Crossed topology of long-gauge strain sensors can be used to monitor shear strain. By an ideal layout of two strain sensors in a planar case, the effect from the normal force, bending moments, and even temperature gradient can be eliminated. However, some slight position changes, e.g., due to on-site conditions, may affect the performance of crossed sensors. Therefore, it is necessary to study the influence of imperfections in the geometrical position of sensors on the measurements of crossed sensors. This paper presents a study on the performance of long-gauge sensors embedded in a spread footing foundation of a five-floor garage at Princeton University. We investigate the effects of topology on the measurement of average shear strain and the relationship between the evaluated shear and loading from the superstructure. The results show that the imperfections in the positioning of sensors have a significant impact on the measurement of shear strain, which needs to be taken into consideration when interpreting the sensor data. The average shear strain evaluated using the crossed sensors measurements is compared with theoretical values obtained from structural analysis. The results validate the estimated relationship between detected strain and applied forces. The findings of this study have important implications for the use of crossed long-gauge strain sensors beyond spread footing foundations, as the method applied here can be extended to other types of structural elements.

## INTRODUCTION

Foundations are crucial to stability of structures and monitoring their behavior is important for detection of malfunction at an early stage. Shear capacity plays important role in guaranteeing stability of Spread Footing Foundation and thus, assessing shear stresses in the footing is of particular interest. However, there are no effective means in monitoring shear stresses, and that is the reason why shear strain is monitored and

Yitian Liang, Branko Glišić, Princeton University, Department of Civil and Environmental Engineering, 59 Olden St, Princeton, NJ 08540, U.S.A.

converted to stresses by using appropriate constitutive equations. Early studies confirmed that strain sensors can be used for evaluating shear strain. Strain gauges combined in various rosette configurations are studied and widely used for this purpose. It was found that the difference in normal strain sensed by any two arbitrarily oriented strain gages in a uniform strain field is proportional to the shear strain along an axis bisecting the strain gage axes [1]. The method was extended to orthotropic, plane-stress case, showing that L-type and V-type gauges could be used to find normal stress $\sigma_x$ and shear strain $\tau_{xy}$ [2].

Hence, these studies, which were in good agreement with classical solid mechanics, prove that combination of strain sensors can be used for monitoring shear strain. However, strain gauges are not applicable in concrete footing due their short gauge length and impractical methods of embedding. Development of embeddable long-gauge fiber optic sensors in the last quarter of century overcame these challenges [3]. These sensors combined in so-called crossed topology were applied in several projects for monitoring average shear strain [3, 4, 5].

However, imperfections in the installation of crossed topology may result in challenges in interpretation and analysis of measurements. In the case of correct sensor placement, typically symmetric with respect to axes of dominant normal stress, the effects from the normal force, bending moment, and even temperature gradient is cancelled, and shear strain simply determined using appropriate expressions. Nevertheless, changes in sensor position, e.g., due to constraints imposed by on-site conditions, affect the measurement results of crossed sensors, and complicate evaluation of shear strain.

The aim of this paper is to carry out preliminary evaluation of the influence of imperfection in geometrical placement of embedded crossed topologies of long-gauge sensors to their performance in shear strain monitoring. Through theoretical derivations, we first established the relationship between the sensor measurements and applied forces. Then, we used monitoring data collected from real structure, Stadium Drive Garage, to validate these relationships and assess performance of imperfectly installed crossed topology of sensors.

## THEORETICAL SOLUTIONS

The measurements of the crossed long-gauge strain sensors depend on the geometric parameters. A literature review has shown no systematic study addressing the alteration in accuracy of the results due to imperfect sensor layout. In order to address this issue, the theoretical expressions for interpretation of crossed sensors measurement as a function of their geometrical position are derived. As a preliminary study we assume that the monitored structural element behaves in accordance with linear beam theory.

The normal strain component at an observed point with coordinates *x* and *y* and in direction of axis *n* in a plane beam case can be written as [6]:

$$\varepsilon_n(x,y) = \frac{\varepsilon_x + \varepsilon_y}{2} + \frac{\varepsilon_x - \varepsilon_y}{2}\cos 2\theta + \frac{\gamma_{xy}}{2}\sin 2\theta \tag{1}$$

where $x$-axis coincides with centroid line of the beam and $\theta$ is the angle between the axis $n$ (describing direction of strain) and the $x$-axis. For prismatic beam with rectangular cross-section the following relationships are valid:

$$\sigma_x(x,y)=\frac{M(x)}{I}y, \tau_{xy}(x,y)=\frac{S(x)}{2I}(\frac{h^2}{4}-y) \tag{2}$$

$$\varepsilon_x(x,y)=\frac{\sigma_x(x,y)}{E}, \varepsilon_y(x,y)=-\nu\frac{\sigma_x(x,y)}{E}, \gamma_{xy}(x,y)=\frac{\tau_{xy}(x,y)}{G} \tag{3}$$

where $h$ is the height (depth) of the cross section and $y$ is the distance from the centroid of the cross-section. Then we can write the strain in the direction $n$ as follows:

$$\varepsilon_n(x,y)=\frac{(1-\nu)+(1+\nu)\cos 2\theta}{2EI}M(x)y+\frac{\sin 2\theta}{2GI}(\frac{h^2}{4}-y^2)S(x) \tag{4}$$

In typical crossed topology one sensor (Sensor 1) is installed in direction $n_1$, with angle $\theta_1$ with respect to $x$-axis, while the other sensor (Sensor 2) is installed in direction $n_2$, with angle $\theta_2$ with respect to $x$-axis. Start points of each sensor are described with their coordinates ($x_1$, $y_1$), ($x_2$, $y_2$), respectively, while coordinates of end points can be determined using start points and corresponding angles $\theta_1$ and $\theta_2$ with respect to $x$-axis. In preliminary analysis, one can consider spread footing foundation as balanced cantilever. For a cantilevered beam under uniformly distributed load, we derive strain field expressions based on Equations 3 and 4, then we integrate the strain along the gauge length of the sensors to obtain estimation of sensor's measurement in the following form:

$$\bar{\varepsilon}=C_M\cdot M+C_S\cdot S+C_q\cdot q \tag{5}$$

where $\bar{\varepsilon}$ is the measured strain which is an average value along the gauge length. $M$, $S$, and $q$ are the bending moment, shear force, and the uniformly distributed load at the start points of sensors. $C_M$, $C_S$, and $C_q$ are all functions of $x_1$, $x_2$, $y_1$, $y_2$, $\theta_1$ and $\theta_2$, which are all geometric parameters of crossed sensors including the position of start points of sensors as well as the angle with the horizontal plane. Evaluation of shear strain is particularly simplified if $\theta_1=-\theta_2$ and further simplified if $\theta_1=\pi/4$. That is the reason why, crossed topology is often installed using these specific angles. In the case of correct sensor placement that we mentioned in Introduction, the subtraction of strain measurements from two sensors is proportional to shear strain and the relationship can be written as [1]:

$$\gamma_{xy}=\frac{\bar{\varepsilon}_1-\bar{\varepsilon}_2}{\sin 2\theta_1} \tag{6}$$

Thus, $S$ is linear related to $\bar{\varepsilon}_1-\bar{\varepsilon}_2$. However, with imperfections in the installation of crossed topology, some effects, e.g., from bending moment, cannot be eliminated, and then the substruction term can be written as follows:

$$\bar{\varepsilon}_1 - \bar{\varepsilon}_2 = (C_M^- \cdot M + C_S^- \cdot S + C_q^- \cdot q) / L_{sensor} \quad (7)$$

where $L_{sensor}$ is the gauge length of the long-gauge strain sensor; sign “minus” in superscript indicates that the corresponding parameters are calculated for subtraction of strain. Similarly, in the case of correct sensor placement, the addition of strain measurements from two sensors is proportional to the bending moment if the normal force and thermal effects are negligible. With imperfections in geometric layout, we can write the formula of addition as:

$$\bar{\varepsilon}_1 + \bar{\varepsilon}_2 = (C_M^+ \cdot M + C_S^+ \cdot S + C_q^+ \cdot q) / L_{sensor} \quad (8)$$

where sign “plus” in superscript indicates that the corresponding parameters are calculated for subtraction of strain. Equations 7 and 8 serve as the basis in evaluation of performance of crossed sensors. They are validated on a real structure as shown in the next section of the paper.

## ON-SITE VALIDATION

Stadium Drive Garage is a five-floor prefabricated assembly structure located in the southeast corner of Princeton University. Two pairs of crossed long-gauge strain sensors, *J1* and *J2*, and two horizontal sensors, *ZS1* and *ZS2*, as shown in Figure 1, were attached to the dummy rebars in a spread footing foundation of the garage before pouring concrete. This section analyzes the strain monitored by crossed sensors *J1S1* and *J1S2* of topology *J1* and the strain monitored by crossed sensors *J2S1* and *J2S2* of topology *J2* during construction, and compares the measurements with the theoretical results.

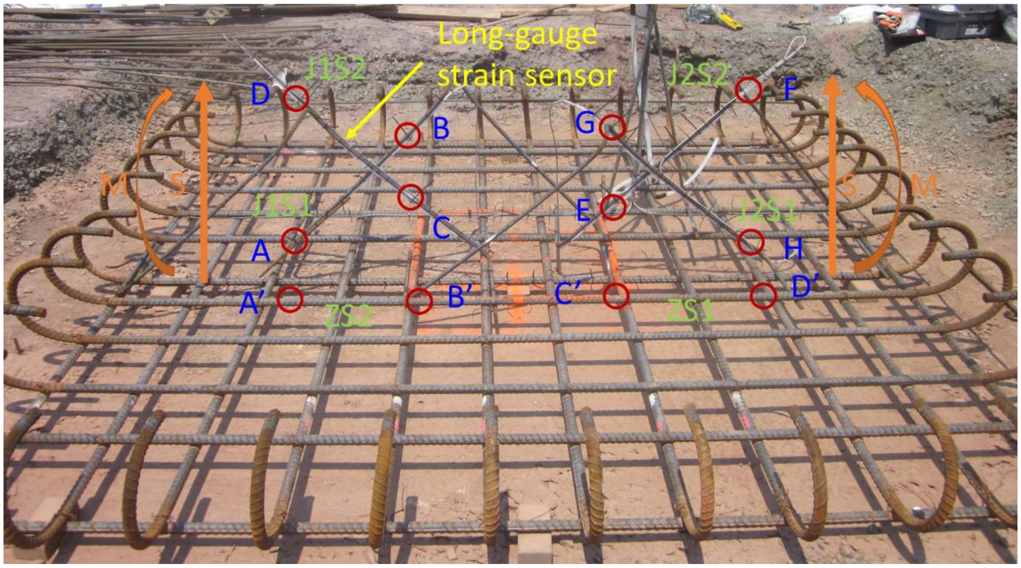


Figure 1. Layout of sensors in the foundation [7].

Based on the geometric layout of *J1* and *J2*, we can calculate the six coefficients in the derived formulars, which are shown in Table I. We can conclude from the values that the effect from shear force *S* dominates the term $\bar{\varepsilon}_1 - \bar{\varepsilon}_2$ and the bending moment *M* dominates the term $\bar{\varepsilon}_1 + \bar{\varepsilon}_2$.

TABLE I. COEFFICIENTS OF J1 AND J2

| **Coefficient** | **J1 x10$^{-12}$** | **J2 x10$^{-12}$** |
|---|---|---|
| $C_M^-$ $(N^{-1})$ | 1.3 | 1.4 |
| $C_S^-$ $(m \cdot N^{-1})$ | 13.6 | 14.4 |
| $C_q^-$ $(m^2 \cdot N^{-1})$ | 0.1 | 0.1 |
| $C_M^+$ $(N^{-1})$ | 10.6 | 11.1 |
| $C_S^+$ $(m \cdot N^{-1})$ | 0.3 | 0.3 |
| $C_q^+$ $(m^2 \cdot N^{-1})$ | -0.2 | -0.2 |

The loads used to compute theoretical results in Figure 4 are evaluated based on the self-weight of superstructure. The beams and slabs of the garage that are supported by the monitored foundation were assembled by a certain order during construction, thus it was possible to estimate approximate values of *M*, *S*, and *q* of *J1* and *J2* in different load cases using the weight of added beams and slabs. After processing the collected sensor data, the theoretical solutions were compared with the on-site monitoring results. Temperature and elastic strain measured during construction are shown in Figures 2 and 3, respectively. Comparison with theoretical solutions is shown in Figure 4. The graphs do not start from zero because the first collected data point in the first stage of construction is used as reference measurement while the average values of all collected data in each stage are used for plots.

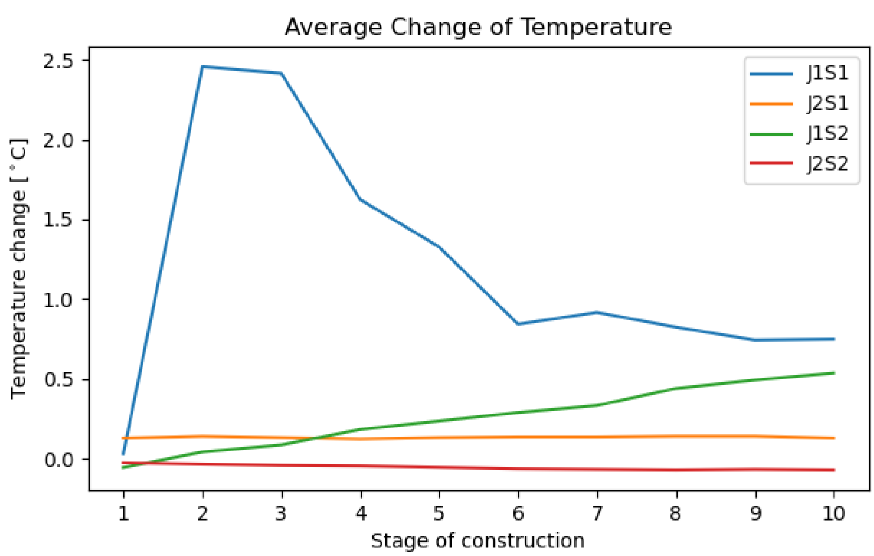


Figure 2. Average change of temperature of four sensors.

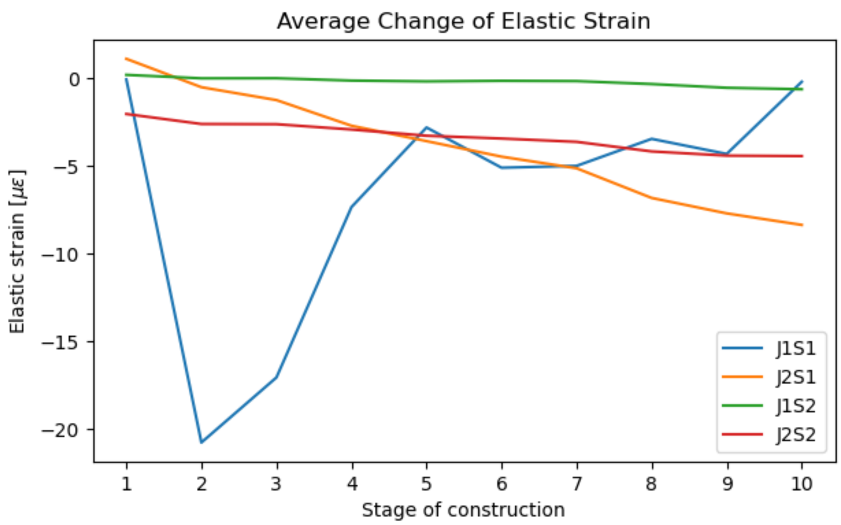


Figure 3. Average change of elastic strain of four sensors.

During the first few stages of construction, the soil above *J2* was in the shadow of the slabs while *J1* was not. This causes only the temperature sensor of *J1S1* to show significant temperature changes in the first 5 stages, which leads to the anomalous strain changes shown in Figure 3 and 4. The beam-column and slab-beam connections are not fixed, and the eccentric force applied to the column has a short offset distance, so theoretically the *M* values of *J1* and *J2* are not large, which causes the lines of *Theory J1* and *Theory J2* in Figure 4 to overlap.

There are significant differences between the theoretical solutions and monitored data in Figure 4. These differences can be explained as follows:

1. The thermal effect. A non-uniform temperature results in deplanation of cross-section of foundation, which in turn leads to discrepancy from solution obtained in linear theory of beam. Figure 2 confirms non-uniform temperature changes; towards the end of construction, as the temperature becomes more uniform, monitoring results reflecting strain difference (see Figure 4a) slowly converge towards the theoretical solutions which is consistent with the assumption that non-uniform temperature is in part responsible for the discrepancy. However, monitoring results reflecting the strain sum are still very different from theoretical solutions, which means that other factors are involved as well.
2. Estimation of parameters. When calculating *M*, *S*, and *q* of *J1* and *J2*, certain model parameters were not available and thus common values were used, e.g., for concrete density and elastic modulus, we used the typical values $\rho=2.4$ $g/cm^3$ and $E=30$ $GPa$. These parameters may not reflect the true parameters of the foundations.
3. Differences between designed and actual structure. Given that discrepancy of strain difference at the end of construction (Figure 4a) is significantly smaller than the discrepancy of sum (Figure 4b), it is likely that the centroid line of foundation is not at the assumed location, i.e., it might be higher than evaluated based on design assumptions. The change in location of centroid line can be result of onset of cracking in concrete.

4. Theoretical assumptions. Plane linear bending and parabolic shear strain distribution might not be accurate for a thick spread footing foundation. And the angles $\theta$ of sensors were not exactly $\pi / 4$.

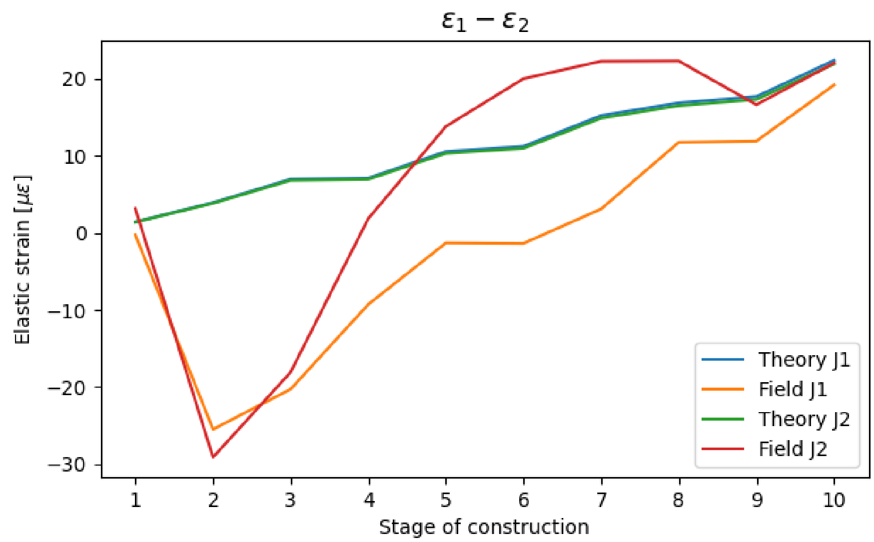


(a)

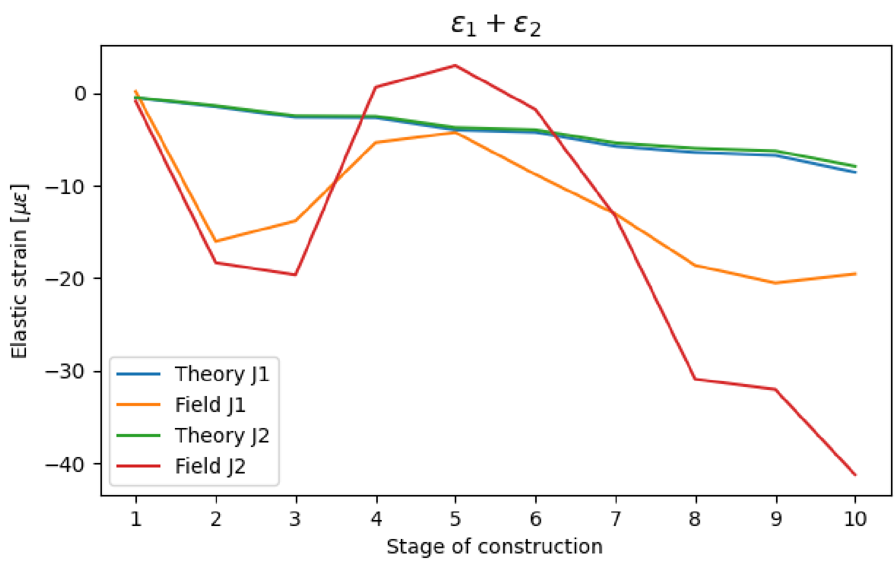


(b)

Figure 4. Comparison between theoretical results and on-site measurements. (a) Substruction of two sensors (b) addition of two sensors.

## CONCLUSIONS

We derived the formulae for $\bar{\varepsilon}_1 - \bar{\varepsilon}_2$ and $\bar{\varepsilon}_1 + \bar{\varepsilon}_2$ theoretically and found that they mainly capture the feature of shear and moment, respectively, but the geometrical layout of sensors still have a significant impact on the measurement, which needs to be considered when interpreting the sensor data. The on-site measurements of a spread footing foundation during construction were compared with theoretical values for validation and it was found that sensors' difference, reflecting the shear strain, is relatively well estimated once the temperature changes become uniform; however, that was not the case with sensors' sum, and various factors that might cause the discrepancy in results were analyzed.

Future work will address the reasons for discrepancy. To minimize effects of non-uniform thermal changes, a short-term loading test will be carried out and collected results will be compared with theoretical values. Sophisticated numerical modelling, i.e., finite element analysis, will be added to predict more accurately theoretical behavior of the foundation. The error propagation due to variation of angle $\theta$ will be analyzed.

## ACKNOWLEDGEMENTS

We would like to thank Gina Talt and Office of Sustainability, Catherine Altadonna and Office of Capital Projects, Dan Polifroni and Whiting-Turner, Mauricio Pereira, and Daniel Trujillo for their help and contribution.

## REFERENCES

1. Perry, C. C.. "Plane-shear measurement with strain gages." Experimental Mechanics 9 (1969): 19N-22N.
2. Bert, C.W. Normal and shear stress gages and rosettes for orthotropic composites. Experimental Mechanics 25, 288–293 (1985).
3. Glišić, B.; Inaudi, D. *Fibre Optic Methods for Structural Health Monitoring*; John Wiley & Sons, Ltd.: Chichester, UK, 2007; ISBN 9780470517819.
4. Kaszubska, Monika et al. "Shear behavior of concrete beams reinforced exclusively with longitudinal glass fiber reinforced polymer bars: Experimental research." Structural Concrete 19 (2018): 152 - 161.
5. Sigurdardottir, D.H.; Glisic, B. On-Site Validation of Fiber-Optic Methods for Structural Health Monitoring: Streicker Bridge. *J. Civ. Struct. Health Monit*. 2015, 5, 529–549.
6. Boresi, Arthur P., and Richard J. Schmidt. *Advanced mechanics of materials*. John Wiley & Sons, 2002.
7. Branko, Glišić. (2023). CEE 537: Structural Health Monitoring [Lecture notes].